AMERICAN SOCIETY of
GENE & CELL
THERAPY

Preclinical Development of Oncolytic Immunovirotherapy for Treatment of HPV^POS Cancers

Lukkana Suksanpaisan,[1] Rong Xu,[2] Mulu Z. Tesfay,[1] Carolyn Bomidi,[1] Stefan Hamm,[2] Rianna Vandergaast,[1] Nathan Jenks,[3] Michael B. Steele,[3] Ayuko Ota-Setlik,[2] Hinna Akhtar,[2] Amara Luckay,[2] Rebecca Nowak,[2] Kah Whye Peng,[3,4,5] John H. Eldridge,[2] David K. Clarke,[2] Stephen J. Russell,[4,5] and Rosa Maria Diaz[4]

[1]Imanis Life Sciences, Rochester, MN 55902, USA; [2]Profectus Biosciences, Inc., Pearl River, NY 10965, USA; [3]Toxicology and Pharmacology Laboratory, Mayo Clinic, Rochester, MN 55905, USA; [4]Vyriad, Inc., Rochester, MN 55902, USA; [5]Deparment of Molecular Medicine, Mayo Clinic, Rochester, MN 55905, USA

Immunotherapy for HPV^POS malignancies is attractive because well-defined, viral, non-self tumor antigens exist as targets. Several approaches to vaccinate therapeutically against HPV E6 and E7 antigens have been adopted, including viral platforms such as VSV. A major advantage of VSV expressing these antigens is that VSV also acts as an oncolytic virus, leading to direct tumor cell killing and induction of effective anti-E6 and anti-E7 T cell responses. We have also shown that addition of immune adjuvant genes, such as IFNβ, further enhances safety and/or efficacy of VSV-based oncolytic immunovirotherapies. However, multiple designs of the viral vector are possible—with respect to levels of immunogen expression and method of virus attenuation—and optimal designs have not previously been tested head-to-head. Here, we tested three different VSV engineered to express a non-oncogenic HPV16 E7/6 fusion protein for their immunotherapeutic and oncolytic properties. We assessed their profiles of efficacy and toxicity against HPV^POS and HPV^NEG murine tumor models and determined the optimal route of administration. Our data show that VSV is an excellent platform for the oncolytic immunovirotherapy of tumors expressing HPV target antigens, combining a balance of efficacy and safety suitable for evaluation in a first-in-human clinical trial.

INTRODUCTION

Overall, 570,000 cases of cancer per year in women and 60,000 cases in men are attributable to human papillomavirus (HPV).[1] Although there have been advances in the treatment of HPV^POS cancers, once first-line treatments fail, patients with metastatic disease generally have few effective treatment options.[2–5] Cancers caused by persistent HPV infection, including cervical, head and neck, anal, vaginal, vulvar, and penile cancers, may be particularly amenable to immunotherapy since the E6 and E7 viral proteins are essential for cancer development, are continuously expressed in >90% of cancer cells, and are absent in normal tissues.[6] Currently, numerous therapeutic vaccines, including live bacteria, viruses, peptides, proteins, and nucleic acids vectors, as well as adoptive T cell therapy, are in clinical development for treatment of HPV-associated cancers. These clinical

studies have demonstrated the generation of E7- and E6-specific T cell immune responses but with limited clinical benefits.[7] HPV^POS cancers have also been treated with checkpoint inhibitors, but response rates are generally less than 20%.[2–5] Therefore, new approaches are needed to alter the immunosuppresive tumor microenviroment for the optimal trafficking and activity of vaccine-induced anti-HPV cytotoxic T cells.

Oncolytic virotherapy constitutes a novel therapeutic strategy, with unique mechanisms of action compared to currently available treatments. Antitumor effects from oncolytic viruses include direct tumor-selective oncolysis, as well as activation of host systemic innate and adaptive immune response.[8,9] Vesicular stomatitis virus (VSV) is a member of the *Vesiculovirus* genus, within the Rhabdoviridae family. The virus is a bullet-shaped, enveloped virus with a single 11-kb negative-strand RNA genome. VSV replicates in the cytoplasm of infected cells, reducing the chances of genetic recombination, has no known transforming potential, and does not integrate any part of its genome into host-cell DNA.[10,11] Recombinant VSV is a potently cytolytic virus with broad spectrum oncolytic activity.[12] The virus can preferentially replicate in many tumor cell types due to defects in interferon (IFN) signaling present in such cells. Extensive proof-of-concept and toxicology studies have been conducted with two VSV variants that have been engineered to express IFNβ.[13–15] One of these VSV variants is currently in a phase 1 clinical trial for treatment of hepatocellular carcinoma and liver metastases of solid tumors (VSV-IFNβ), and a second vector is in a phase 1 clinical trial for refractory solid tumors, hematological malignancies, and endometrial cancer (VSV-IFNβ-NIS).

A previous report showed the feasibility of using an attenuated VSV expressing HPV E7 protein as a platform for therapeutic vaccination

against HPV[POS] tumors in mice.[16] It has also been shown that the expression of a tumor-associated antigen by oncolytic VSV increased the level of tumor-antigen-specific T cell activation, which translated into increased antitumor therapy.[17–19] In addition, HPV genes expressed by a VSV-related *Vesiculovirus* named Maraba virus efficiently boosted HPV-specific immune responses primed with an adenovirus vaccine expressing the same HPV proteins.[20] We decided to combine the oncolytic and vaccine properties of VSV by incorporating a gene encoding tumor-specific antigen(s) into the virus genome. We hypothesized that the "hot" tumor microenvironment generated by the inflammatory cell killing by VSV would allow optimal trafficking and activity of tumor-specific cytotoxic T cells, which is lacking in current therapeutic HPV vaccine approaches.

Collectively, these findings indicate the potential of using virally expressed E6 and E7 proteins as immunotherapy of HPV[POS] cancers. The goal of the current study was to compare different VSV vector designs in order to identify a clinical candidate having optimal efficacy and toxicity profiles, in addition to identifying an optimal route of virus administration. Therefore, we compared three different VSV-derived immunovirotherapy vectors expressing a non-oncogenic form of HPV16 E7/6 fusion protein for efficacy and toxicity. In particular, we chose different designs of vectors in which the position of the immunogenic transgene may affect levels of antigen expression, and we used alternative strategies to attenuate viral pathogenicity. We used two different syngeneic tumor mouse models (HPV[POS] TC-1 and HPV[NEG] MPC-11) specifically to assess both the immunotherapeutic and direct oncolytic activities of the candidate vectors. As a result of the studies reported here, we have selected a candidate vector for translation to a first-in-human clinical trial using a VSV platform targeting HPV[POS] cancers.

RESULTS

Characterization of Different VSV Expressing E7/6

To exploit the therapeutic potential of oncolytic VSV by combining cell killing with specific boosting of antitumoral immunity, we generated a panel of different VSVs encoding a mutated HPV fusion E7/6 protein to determine the optimal design for clinical use. HPV16 is believed to be responsible for approximately 52% of all cervical carcinomas[21] and accounts for 90% of HPV-induced head and neck cancers.[22–24] Wild-type E6 and E7 proteins of high-risk HPV16 are oncogenes. Therefore, based on previously described studies,[25–27] five different mutations (PM [penta-mutant]) were introduced in the HPV16 E7/6 PM fusion protein abrogating the oncogenic potential of the corresponding wild-type proteins[28] by disrupting specific interactions with p53 and retinoblastoma tumor suppressor proteins. Three amino acid changes affect both zinc-finger domains in the E6 protein and the single zinc-finger domain in the E7 protein, respectively. Two additional mutations destroy the pRb binding domain in the E7 protein.

In VSV-E7/6-N4CT9 (Figure 1A), the fusion protein gene was inserted at the first position in the viral genome, enabling maximum E7/6 mRNA transcription (due to the fact that VSV gene transcription is attenuated at downstream positions) and expression.[29] This

virus was also attenuated by combining N gene translocation to position 4 in the viral genome with G gene truncation.[30] The mutant M protein in VSV-M51R-E7/6 has a decreased ability to inhibit host cell antiviral mechanisms, allowing the expression of type I IFN, which is a potent VSV inhibitor, thereby helping to protect normal cells from cytolytic damage by the virus.[31–33] VSV-E7/6-mouse and human (m/h)IFNβ has an intact viral M protein and incorporates the mouse or human IFNβ gene,[34] which results in rapid and robust expression of this cytokine. Expression of the E7/6 protein fusion following infection of baby hamster kidney (BHK-21) cells, which are routinely used for production of VSV, with each viral stock was confirmed by western blot (Figure 1B).

Most of the viruses propagated on BHK-21 cells with similar kinetics to a control VSV expressing GFP, generating high virus titers and peaking at 24 hr post-infection (hpi) (Figure 1C). VSV-E7/6-N4CT9 replication was slower, generated lower titers, and peaked at 48 hpi at a level that was approximately 100-fold lower than the other viruses. In murine tumor TC-1 cells (Figure 1D), VSV-E7/6-N4CT9 replication was slower than the other viruses but reached similar peak levels at 48 hpi. VSV-E7/6-mIFNβ replication in TC-1 cells was comparable to the other viruses at 12 hpi; however, additional virus replication after 12 hr was then abrogated, presumably due to the sensitivity of the TC-1 cells to the mIFNβ expressed by the virus.

All viruses showed similar oncolytic activity at a MOI of 10 in TC-1 cells (Figure 1E). At MOIs of 0.1 and 1, VSV-E7/6-mIFNβ exhibited significantly reduced TC-1 killing activity. In highly VSV-susceptible murine plasmacytoma MPC-11 cells[35] (Figure 1F), all viruses exhibited robust cell killing activity at all MOIs, except for VSV-E7/6-N4CT9, which killed only ~70% of the cells at the lowest (0.01) MOI tested.

Efficacy and Safety Studies in Mice

The therapeutic effect of the different VSV expressing E7/6 was tested in the TC-1 tumor model, which expresses both HPV16 E7 and E6 proteins as target immunogens.[36] As shown in Figure 2, all VSV-E7/6 tested were therapeutically effective after intravenous (i.v.) or intratumoral (i.t.) administration as compared to mice treated with saline or with a control VSV expressing an irrelevant antigen (NY-ESO-1). These results suggested that an effective immune response against E7 and E6 was generated by administration of different VSV-E7/6 vectors. In support of this hypothesis, splenocytes from surviving mice tested positive in an enzyme-linked immunospot (ELISPOT) assay for anti-E7- and -E6-specific T cell responses (Figure 2C). Splenocytes from control mice at the time of sacrifice (due to tumor burden) didn't generate any detectable anti E7 and E6 T cell responses when tested by the same ELISPOT assay.

The fact that VSV-NY-ESO-1 did not show any efficacy suggested that the therapeutic activity of VSV-E7/6 in the TC-1 model was principally due to the induction of an HPV-specific immune response. Therefore, to compare the direct oncolytic activity of the vectors, we also tested the efficacy of the VSV-E7/6 vectors in the HPV[NEG]
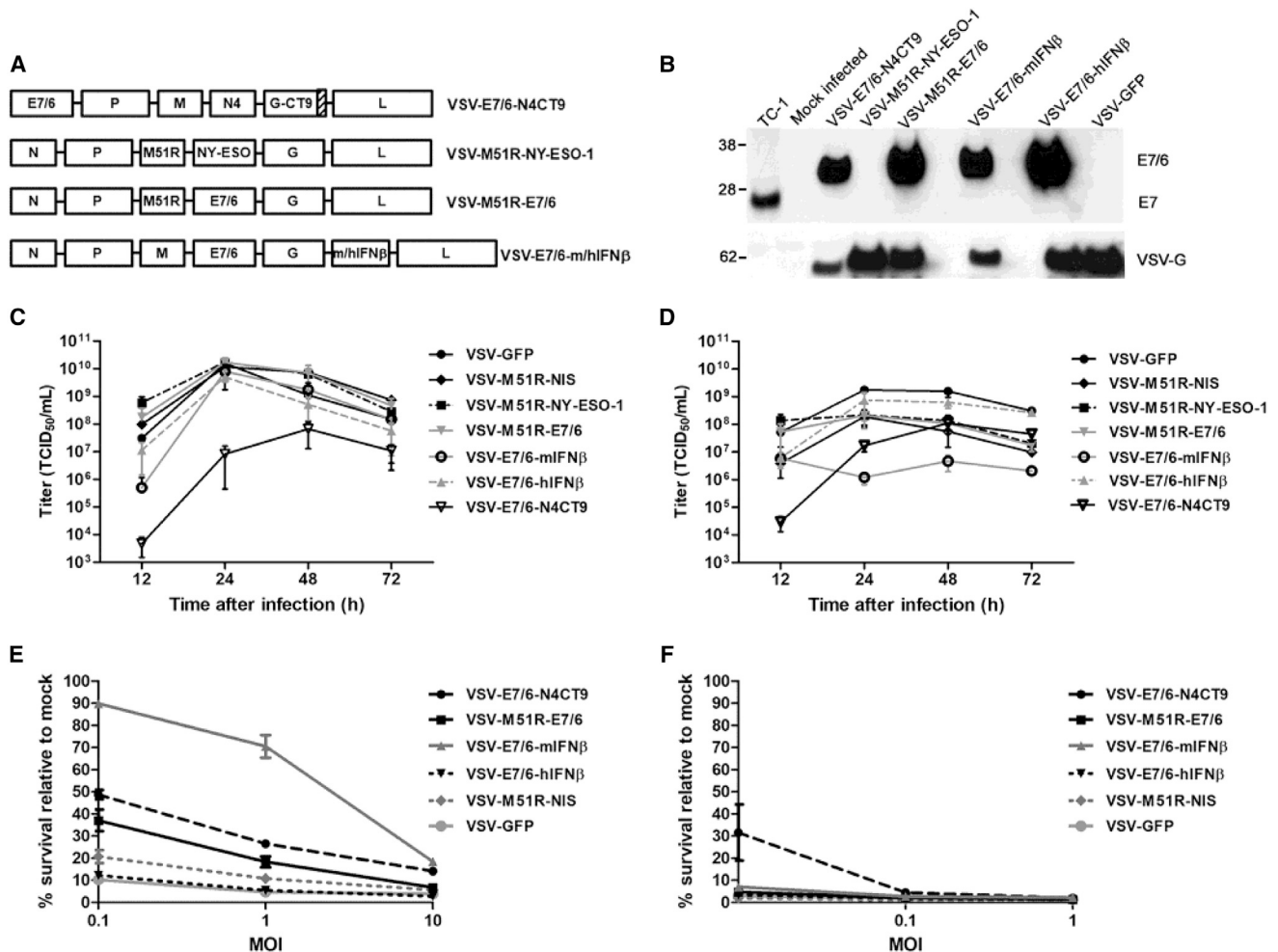
Figure 1. Characterization of VSV Expressing E7/6 Fusion Protein

(A) Genome organization of VSV vectors expressing HPV16 E7/6. (B) E7/6 fusion (top row) and VSV-G (bottom row) protein expression was assessed by western blot. BHK cells were infected with indicated viruses at a MOI of 3. A wild-type E7-expressing TC-1 cell line was used as a positive control (top row). Viral growth curves on (C) BHK-21 and (D) TC-1 cells infected at a MOI of 0.002 and 0.1, respectively. *In vitro* cytotoxic activity of VSV in (E) TC-1 and (F) MPC-11 murine tumor cell lines. An MTS cell-viability assay following infections with increasing MOIs were performed at 48 hr after infections. Error bars, SD of the mean.

MPC-11 murine plasmacytoma model, which is highly susceptible to oncolytic VSV. Even a low dose of virus can lead to extensive intra-tumoral viral replication, sustained viremia, intravascular coagulation, and a rapidly fatal tumor lysis syndrome (TLS).[35]

Despite the fact that VSV-E7/6-mIFNβ was most potent at suppressing tumor growth when given i.t. or i.v. (Figures 3A and 3B), mice treated with this virus showed significant weight loss (>20%), were moribund or lethargic, and were accordingly euthanized early (five mice in the i.t. group and six mice in the i.v. group). To evaluate survival independent of toxicity, mice from these groups were omitted from the Kaplan-Meier survival analysis (Figures 3C and 3D). Survival of those mice treated with VSV-E7/6-mIFNβ, in which there was no observed toxicity, was significantly extended compared to control mice (p = 0.0243 i.v. and p = 0.0034 i.t.).

Mice treated with VSV-M51R-E7/6 survived significantly longer than saline-treated controls (Figure 3C, p = 0.0021, and Figure 3D, p = 0.04), irrespective of the route of administration. Even though VSV-E7/6-N4CT9 demonstrated significant therapeutic efficacy when administered i.t. (Figure 3D; p = 0.0099), mice treated i.v. with this virus did not show prolonged survival compared to saline control (Figure 3C; p = 0.0865). The opposite situation was observed with VSV-E7/6-hIFNβ, which demonstrated efficacy when given i.v., but not i.t. (Figure 3C, p = 0.0154, and Figure 3D, p = 0.3162). Importantly, no toxicities were associated with these three viruses in contrast to VSV-E7/6-mIFNβ therapy.

Because many of the VSV-E7/6-mIFNβ treated mice were euthanized due to toxicity (inactivity, lethargy, or >20% weight loss), blood was collected from these mice. Most notably, the lymphocytes and platelet
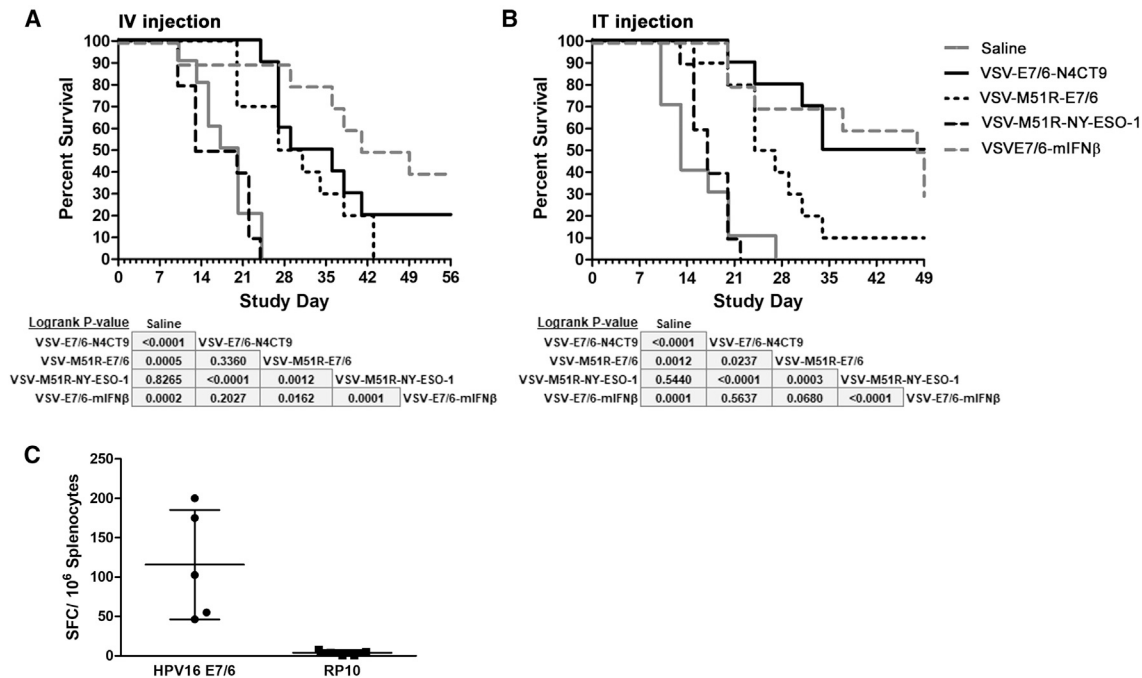
Figure 2. Efficacy of VSV-E7/6 Vectors in the Murine TC-1 Tumor Model

Kaplan-Meier survival curve of C57BL/6 mice (n = 10) bearing TC-1 tumors following three virus doses, injected either i.v. (5×10^8 $TCID_{50}$) or i.t. (4.2×10^8) every other day (A and B, respectively) starting 7 days after tumor implantation. Kaplan-Meier survival curves were compared by log rank (Mantel-Cox) analysis. A value of p < 0.05 was considered statistically significant. (C) HPV16 E7/6 specific T cell response detected by ELISPOT assay in surviving mice (VSV-M51R-E7/6 group), following restimulation of splenocytes with either medium alone or a pool of overlapping E7 and E6 mixpeptides. Error bars, SD of the mean.

counts of i.v. VSV-E7/6-mIFNβ treated mice were lower compared to those of the other groups (Figure 4A). Blood urea nitrogen (BUN), alkaline phosphatase (ALP), and alanine aminotransferase (ALT) levels in mice treated either i.t. or i.v. with VSV-E7/6-mIFNβ were also elevated compared to other mice in the other treatment groups (Figure 4B).

Because VSV-M51R-E7/6 treatment was effective in HPV^{POS} and HPV^{NEG} tumor models without toxicity, we characterized this virus further by increasing the dose and frequency of viral injections. As shown in Figure 5A, increasing the viral dose 100-fold and the frequency of administration to three doses didn't generate toxicity while demonstrating significant survival compared to control mice (p = 0.0021 for i.t., p < 0.0001 for i.v.). To further support the safety profile of this virus, *in vitro* killing activity of VSV-M51R-E7/6 (Figure 5B) was comparable to VSV-GFP in different human tumor cell lines (HT1080, fibrosarcoma; Mel624, melanoma; LoVo, colorectal), while having minimal cytotoxic activity in a normal primary human cell line (HEKa, human epithelial keratinocytes).

Optimizing VSV-M51R-E7/6 Administration

Based on the observation that the therapeutic effect seen in the TC-1 tumor model with VSV-M51R-E7/6 was largely dependent on its immunizing properties and that a VSV encoding Zaire Ebola virus surface glycoprotein administered by the intramuscular (i.m.) route has demonstrated clinical efficacy as an Ebola vaccine,[37] we evaluated

the immunotherapeutic activity of VSV-M51R-E7/6 in the TC-1 tumor model when virus was given by i.m. and i.v. routes. Treatment with virus significantly delayed tumor growth (Figure 6A) and increased survival in all groups compared to control mice (Figure 6B). Virus delivered i.v. resulted in prolonged survival compared to virus delivered i.m. (p = 0.0599), suggesting that systemic delivery is superior to local i.m. delivery for the generation of a potent antitumoral immune response. Notably, as shown in Figure 6C, four i.v. doses of VSV-M51R-E7/6 did not enhance survival compared to a single i.v. dose in the TC-1 tumor model.

Because only one i.v. dose of virus was necessary for significant therapy, we evaluated the combination of a single i.v. dose followed by, or simultaneously with, an i.t. dose(s). Figure 6D shows that all combinations tested were effective in increasing mouse survival when compared with the control group, and although the median survival for i.t. dosing only was 21 days, the median survival for the other two treatment groups tested was not reached.

VSV-M51R-E7/6 Immunovirotherapy Is Dependent on a CD8$^+$ T Cell Response

Seven days after VSV-M51R-E7/6 administration, we observed very extensive leukocytic infiltration into all VSV-treated tumors compared with the control saline-treated group. Furthermore, viral treatment resulted in an increased influx of total CD3$^+$ T cells,
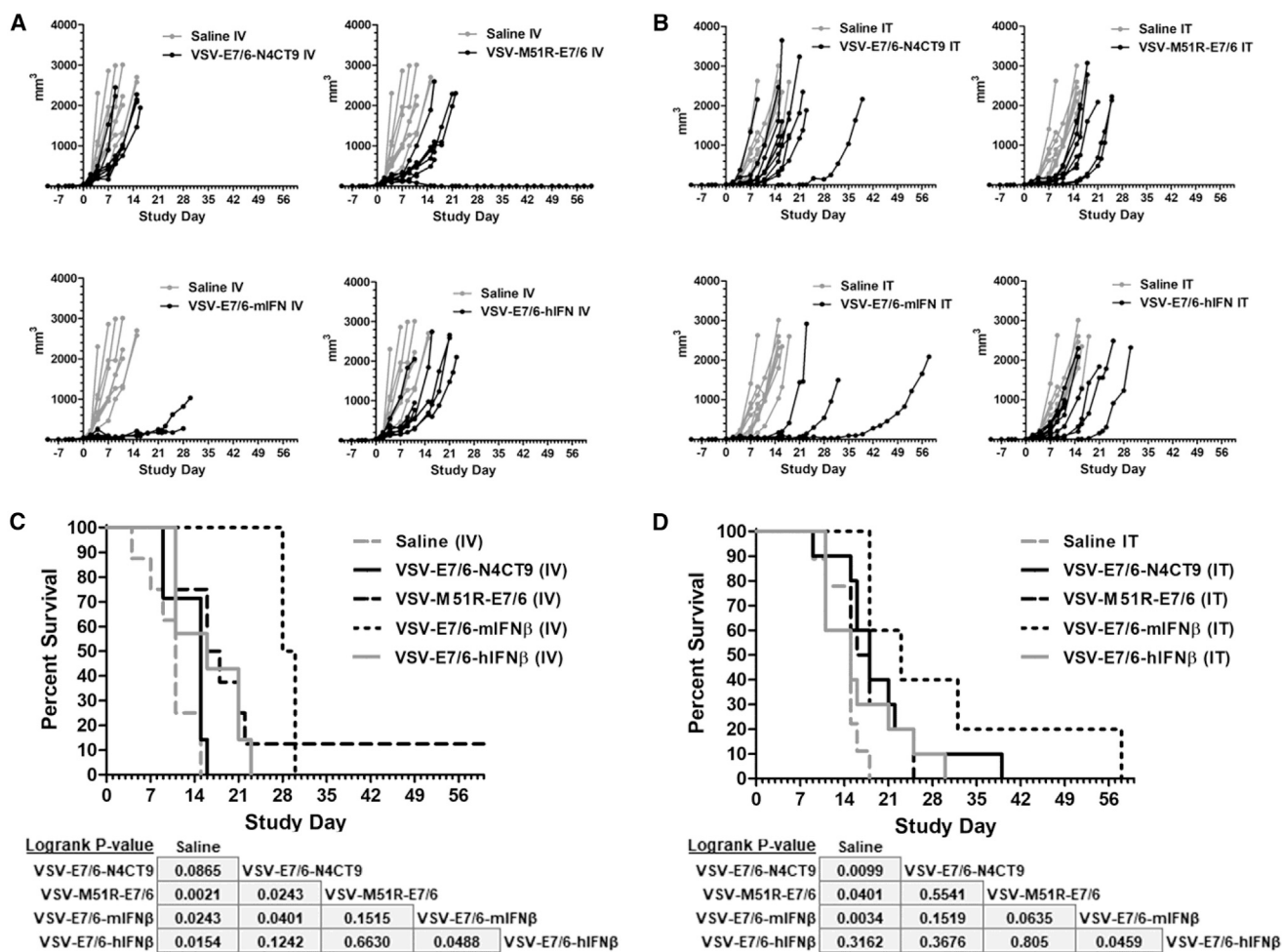
Figure 3. Efficacy and Toxicity of VSV-E7/6 Vectors in the Murine MPC-11 Tumor Model

Tumor volume measurements of BALB/c mice (n = 10) bearing MPC-11 tumors after treatment with either a single i.v. (A) or i.t. (B) injection of virus (5×10^6 TCID$_{50}$) on day 7 after tumor implantation. Kaplan-Meier survival curve of the same groups of mice after i.v. (C) or i.t. (D) viral administration. A value of p < 0.05 was considered statistically significant.

including CD8$^+$ and CD4$^+$ T cells (Figure 7A). These results suggest that the therapeutic effect seen with this virus may be the result of host-derived immune effectors specific for tumor-associated antigens.

All mice treated with VSV-M51R-E7/6 had significantly increased levels of specific T cell responses against the E7 and E6 tumor antigens and viral N protein, consistent with reduction in tumor volumes (Figures 7B and 7C), further supporting the role of an immune response in the efficacy of VSV treatment in these mice. To better understand the role of these immune effectors *in vivo*, immunovirotherapy was performed in mice previously depleted of CD4$^+$, CD8$^+$, or natural killer (NK) cells (Figure 8). In mice depleted of CD8$^+$ T cells, there was a complete abrogation of VSV-M51R-E7/6 therapy. In contrast, we did not observe highly significant differences in the rate of tumor growth in CD4$^+$-T cell- or NK-cell-depleted mice compared to non-

depleted mice, suggesting that these cell subtypes do not mediate the antitumor effects observed.

DISCUSSION

Cancer immunotherapy and oncolytic virus therapy are rapidly emerging modalities offering the potential for clinical benefit when other therapies become ineffective. By modifying oncolytic viruses to express tumor-specific antigens, both therapeutic approaches can be combined to potentiate direct tumor destruction and induction of durable and efficacious antitumoral immune responses,[38] a feature that is lacking in the vast majority of current viral vector-based HPV cancer vaccines.[7] Proof-of-concept studies have previously determined that HPV^{POS} cancers can be targeted therapeutically when HPV E7 and/or E6 proteins are expressed by VSV or another VSV-related vector.[16,20] However, to our knowledge, we describe here the first study comparing different vector designs and routes of
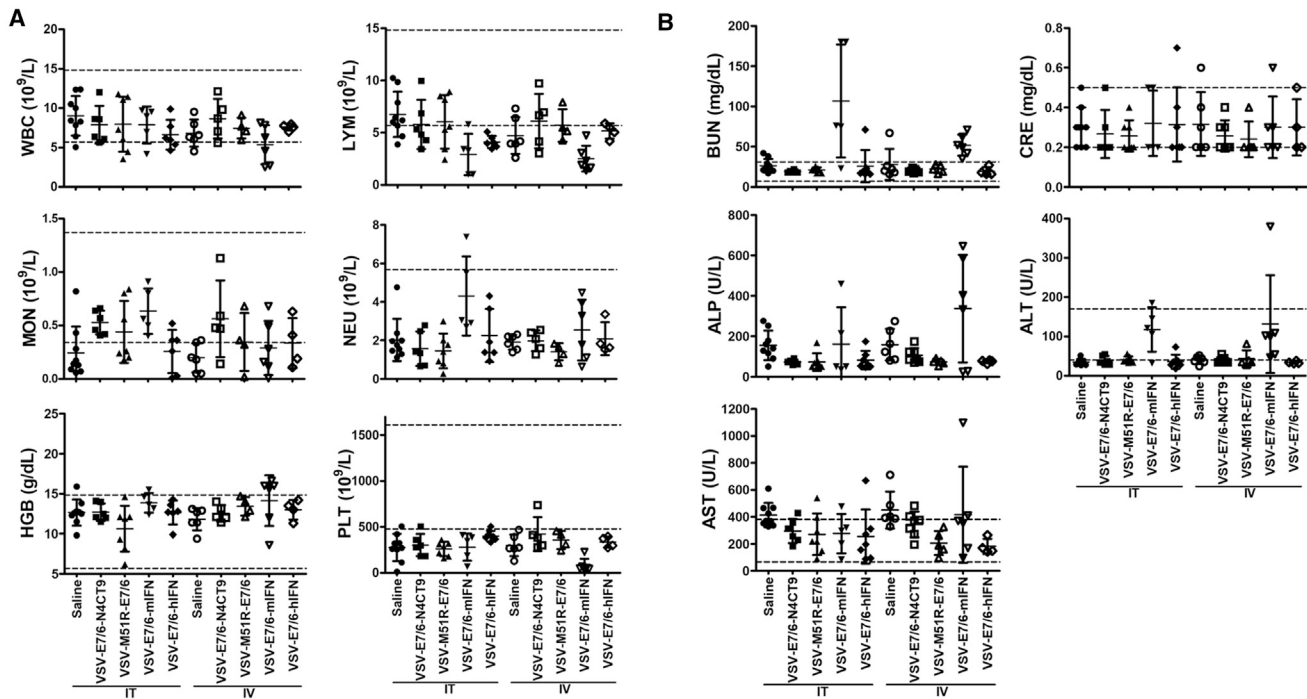
Figure 4. Profiles of Blood and Liver Function Enzymes in MPC-11 Tumor-Bearing Mice after Treatment with VSV-E7/6 Vectors

(A) At the time of euthanasia in saline or treatment groups, blood was collected by retro orbital bleed to monitor changes in blood composition; WBC, total white blood cell; LYM, lymphocyte; MON, monocyte; NEU, neutrophil; HGB, hemoglobin; PLT, platelet. The dot lines indicate the 95% interval of each parameter measure in 158 normal 8- to 10-week-old female BALB/c mice. (B) Profiles of liver function enzymes at the time of euthanasia in saline or treatment groups. Blood was collected by retro orbital bleed to monitor liver function; BUN, blood urea nitrogen; CRE, creatinine; ALP, alkaline phosphatase; ALT, alanine aminotransferase; AST, aspartate aminotransferase. The dotted lines indicate the 95% interval of each parameter measured from 121–133 normal 8- to 10-week-old female BALB/c mice. Error bars, SD of the mean.

administration in order to develop a clinical product and dosing regimen with optimal efficacy and safety profiles.

We mutated the E7/6 fusion protein to minimize the known oncogenic potential of the corresponding wild-type proteins. In addition, the use of a VSV delivery platform presents an additional and probably even more important safety feature. VSV transcribes and replicates exclusively in the cell cytoplasm and does not involve any DNA intermediates. Therefore, there is a low risk of the HPV antigen-encoding RNA sequences becoming incorporated into the host cell genomic DNA. In addition, the strong VSV-induced cytopathic effect will kill infected cells, effectively preventing development of the transformed phenotype.

The three different VSV vectors were attenuated either by N gene translocation in combination with a G protein cytoplasmic tail truncation,[30] by mutation of amino acid 51 in the M gene,[33] or by expression of IFNβ.[34] Cancer cells are often hyporesponsive to IFNβ, allowing the viral infection to spread more efficiently in cancerous tissue, where it is selectively destructive (oncolytic). Moreover, IFNβ has antitumor effects, including enhancement of innate immune responses, antiproliferative activities, and the priming of T cell responses.[39] Indeed, STING agonists currently developed as cancer immunotherapy act by stimulating IFNβ production.[40] Each of the

three vectors was also modified to express a HPV16 E7/6 fusion protein that was modified to eliminate the oncogenic potential associated with natural forms of E7 and E6.

All of the VSV vectors showed similar levels of viral replication and oncolytic activity *in vitro* and were therapeutically effective against syngeneic TC-1 HPV16-positive tumors after i.v. or i.t. administration. Significantly, however, in the TC-1 model, an oncolytic VSV expressing an irrelevant antigen (VSV-NY-ESO-1) lacked any therapeutic effect, indicating that efficacy was mediated by E7 and E6 immune responses (Figure 2). This hypothesis was supported by the detection of E7- and E6-specific T cell responses in splenocytes harvested from VSV-E7/6-treated mice, the accumulation of leukocytes and CD8+ T cells at tumor site(s) and the abrogation of efficacy when CD8+ T cells were specifically depleted during VSV-E7/6 treatment (Figures 7 and 8). Interestingly, we did not see highly significant contributions of either CD4+ T or NK cells to efficacy (Figure 8). Of particular note, we observed that i.t. virus administration, combined with i.v. administration, generated a trend toward increased intratumoral leukocyte infiltration compared to either administration alone (Figure 7A). Since our data also show that a combination of antiviral and antitumor T cells is induced by our treatment protocols (Figure 7B) and yet the VSV-NY-ESO-1 virus lacked efficacy (see above), we believe that anti-E7 and -E6 CD8+ T cells are the major
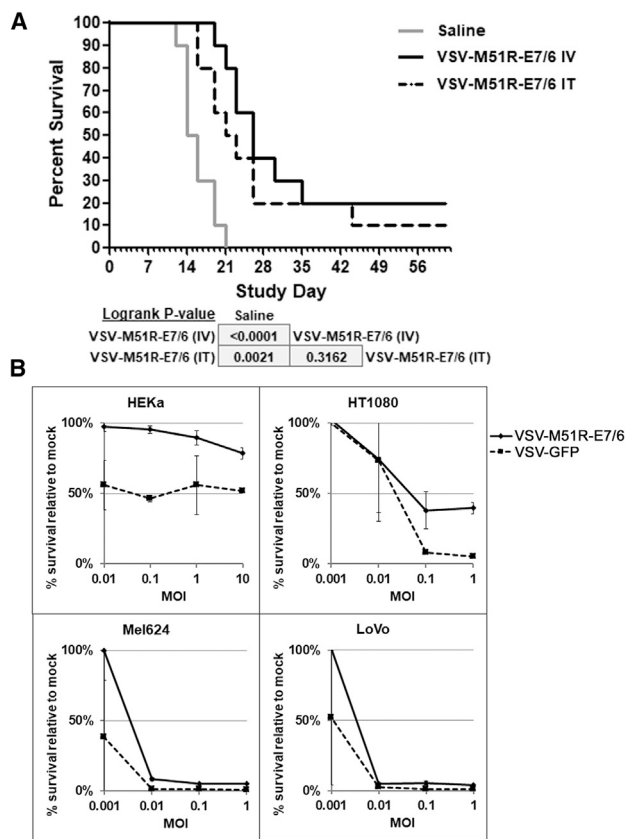
Figure 5. In Vivo and In Vitro Efficacy and Safety following Multiple Administrations of VSV-M51R-E7/6 and In Vitro Cytotoxic Effect on Human Cells

(A) Kaplan-Meier survival curve of BALB/c mice (n = 10) bearing MPC-11 tumors after treatment with three doses of VSV-M51R-E7/6 (5×10^8 TCID$_{50}$/dose), injected either i.t. or i.v. every other day, starting 7 days after tumor implantation. p < 0.0001 (saline versus i.v. injection); p = 0.0021 (saline versus i.t. injection) Kaplan-Meier survival curves were compared by log rank (Mantel-Cox) analysis. A value of p < 0.05 was considered statistically significant. (B) In vitro cytotoxic activity of VSV-M51R-E7/6 in a panel of human cell lines. The indicated cell monolayers were infected with VSV-M51R-E7/6 (solid line) or VSV-GFP (dotted line) at the indicated MOIs. An MTS cell viability assay was performed 72 hr post-infection. HEKa, normal primary epidermal keratinocytes; HT1080, fibrosarcoma; Mel624, melanoma; and LoVo, colorectal adenocarcinoma. Error bars, SD of the mean.

contributor to therapy in this TC-1 model. Notably, none of the VSV demonstrated any significant toxicity by any of the administration routes, indicating the different specific attenuation mechanisms were operating in the TC-1 mouse model.

We also compared the efficacy and/or toxicity profiles of our candidate viruses in a tumor model where direct oncolytic effects of the viruses would be more clearly manifested. In this respect, the mouse MPC-11 plasmacytoma model is ideal for testing VSV oncolytic activity and toxicity.[35] MPC-11 cells do not express HPV16 proteins. Therefore, any therapeutic effects with VSV expressing HPV E7/6 would be most likely attributable to direct oncolytic effects. When

therapy was given as a single low dose of 5×10^6 tissue culture infective dose (TCID$_{50}$), VSV-E7/6-mIFNβ (Figure 3) was the most effective but at the cost of high toxicity in almost half of the treated mice (significant weight loss, decrease in lymphocyte count and platelet count, and increase in liver enzymes). The analogous vector expressing human IFNβ, which is not functional in mouse cells, showed no such toxicity. A recent preclinical study also confirmed the toxicities associated with high circulating levels of IFNβ,[35] which were minimized with the administration of the JAK 1 and 2 inhibitor ruxolitinib (K.W.P., unpublished data).

Since there was little difference in the degree of tumor control among the vectors expressing the fusion protein E7/6 in the TC-1 model, final selection of the M51R-E7/E6 vector was based on the favorable balance of efficacy and safety when testing its oncolytic activity in the highly susceptible MPC-11 model. The M51R mutation renders the virus less efficient in shutting down host cell innate responses to infection,[33] resulting in the production of type I IFN. The less-efficacious vectors in the MPC-11 model were VSV-E7/6-N4CT9, which was originally developed as a highly attenuated replication competent vaccine[30] (Figure 1), and VSV-E7/6-hIFNβ with an intact M and expressing human IFN, which is inactive in mice. We also showed efficacy and a lack of toxicity with higher doses of VSV-M51R-E7/6 virus in the HPV^{NEG} MPC-11 model (Figure 5A), further demonstrating the direct oncolytic properties of the virus.

Taken together, these data indicated that VSV-M51R-E7/6 therapy provides the optimal balance of efficacy and safety. In addition, our studies have clearly shown the value of comparing the design of vectors within a virus type. This will allow for a rational selection of the optimal vector design to ensure the best backbone of efficacy and safety for clinical translation. Therefore, this vector was then selected to define an optimal route of administration. Typically, VSV vectors used in clinical trials as antipathogen vaccines have been administered i.m. because of the requirement for minimal vector dissemination.[41,42] In contrast, a VSV-related recombinant Maraba virus has only been administered i.v. as an oncolytic agent and to boost tumor-specific immune responses in cancer clinical trials (NCT02285816 and NCT02879760). Hence, we tested the effectiveness of i.m. viral delivery in the context of a tumor model. Our data indicated tumor control in the TC-1 model was immune mediated, and systemic (i.v.) administration of the virus was significantly superior to i.m. delivery, presumably because of more rapid and robust dissemination in the blood to the spleen and lymph nodes.[43]

Repeated administration of viral vectors as either oncolytic agents or vaccines may be limited by the generation of antiviral neutralizing antibodies.[44–47] Consistent with this, we observed that repeat dosing with VSV-M51R-E7/6 was no better than a single dose in conferring significant mouse survival (Figure 6C). In this study, we have compared different vectors of the same virus type. These results complement those of Atherton et al.,[20] who showed that a heterologous prime-boost strategy with different viral vectors can considerably
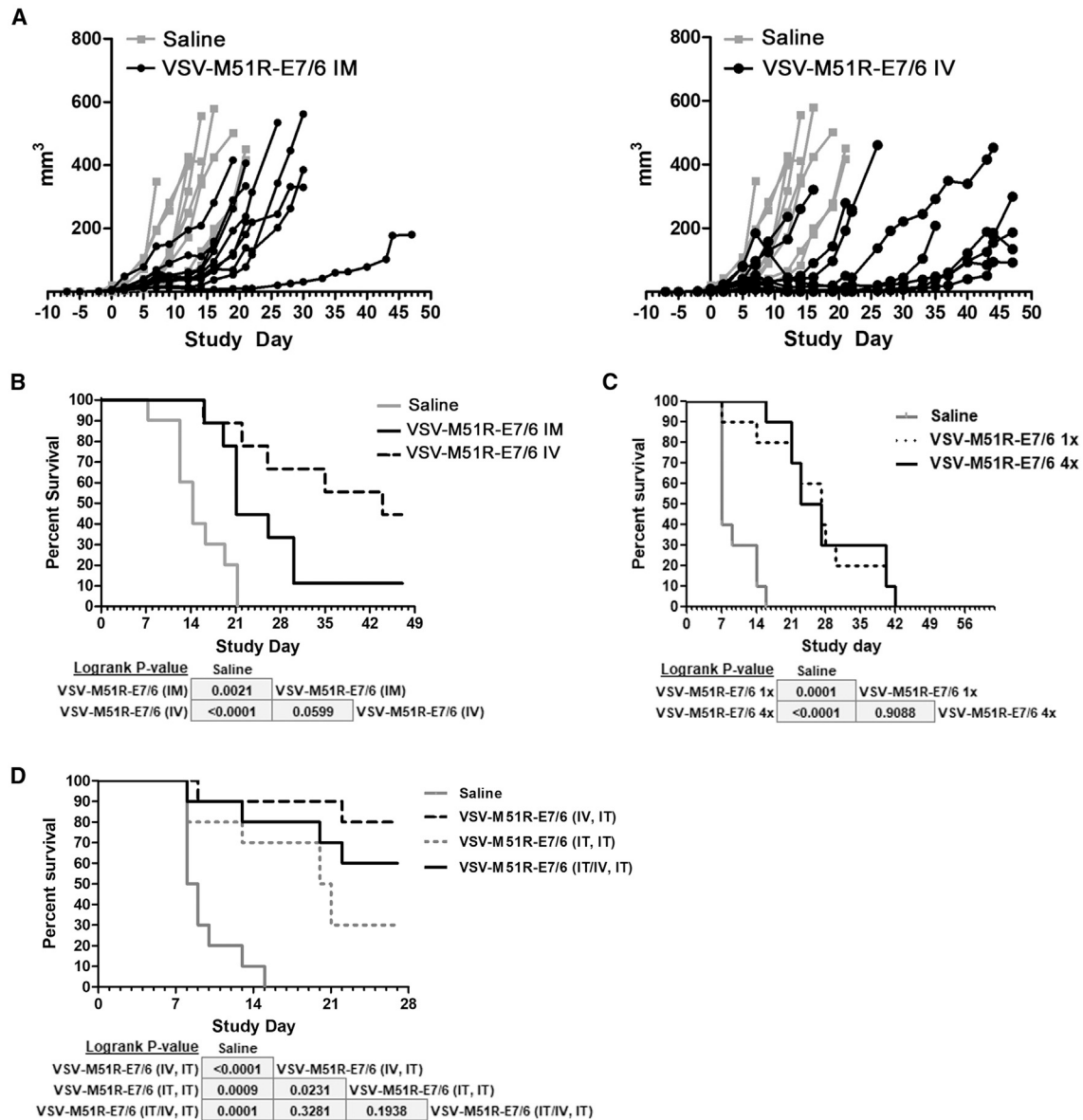
Figure 6. Optimizing Route of Administration and Dosing Schedule of VSV-M51R-E7/6 Therapy

(A) Tumor volumes of C57BL/6 (n = 10) mice bearing TC-1 tumors after treatment with either four i.m. (left) or i.v. (right) VSV-M51R-E7/6 (5×10^8 TCID$_{50}$/injection) injections every other day. (B) Corresponding Kaplan-Meier survival curve of mice treated with VSV-M51R-E7/6 by i.m. or i.v. injections. (C) Kaplan-Meier survival curves of mice treated with either one or four i.v. injections of VSV-M51R-E7/6 (5×10^8 TCID$_{50}$/injection). (D) Kaplan-Meier survival curve of mice after treatment with either a single i.v. or i.t. injection or following concomitant i.v. and i.t. injection with VSV-M51R-E7/6 (5×10^8 TCID$_{50}$ total dose in each case, splitting the dose in half for concomitant i.v. and i.t. administration) starting 7 days after tumor implantation. An additional i.t. dose (5×10^8 TCID$_{50}$) was given to all groups 10 days after the first injection. Kaplan-Meier survival curves were compared by log rank (Mantel-Cox) analysis. A value of p < 0.05 was considered statistically significant.

improve therapy in the TC-1 model. Another study[48] found that the combination of cisplastin followed by i.t. injection of a vaccinia vector expressing HPV proteins generated a potent therapeutic effect in the same murine model. However, in our study, a combination of i.v. and i.t. routes of administration with VSV-M51R-E7/6 generated optimal therapy under the conditions that we used in the TC-1 model. We believe that the first i.v. dose allows optimal systemic delivery prior to the development of anti-VSV immunity. This initiates an effective systemic antitumoral response. Simultaneous and subsequent i.t. dosing further provides a localized oncolytic effect, which can be repeated to control individual lesions. Concomitant i.v. and i.t. administration at day 1 using a split dose should help ensure viral infection and spread occurs simultaneously in locally injected and distant tumors.

A

Total Leukocytes

Total T Cells

CD8+ T Cells

CD4+ T Cells

B

HPV16 E7E6

VSV N

C

Day 20 Tumor Vol.

* p < 0.05
** p < 0.01
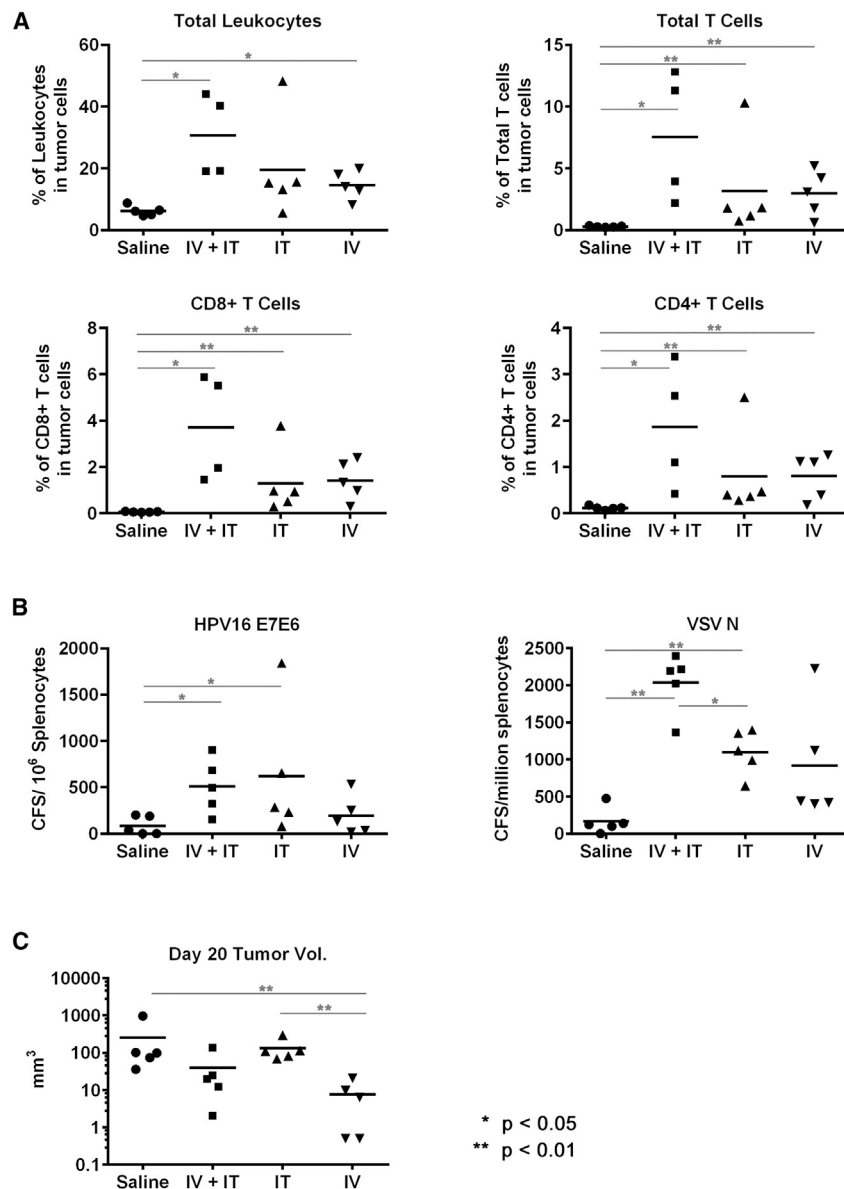
Figure 7. Effect of VSV-M51R-E7/6 Administration on the Tumor Microenviroment and Generation of Antigen-Specific T Cell Immune Responses

(A) TC-1 tumors (n = 5) were harvested 7 days after viral therapy and analyzed by flow cytometry. (B) Mouse IFNγ ELISPOT assay was performed on splenocytes (n = 5) harvested 20 days after viral administration. (C) Tumor volume measurements at day 20 after i.t., i.v., or concomitant i.v. + i.t. administration of VSV-M51R-E7/6 (5×10^8 $TCID_{50}$ total dose, splitting the dose in half for concomitant i.v. + i.t. injection) starting 7 days after tumor implantation. The data shown are the average of experiment with five mice per group. p values were calculated using non-parametric Mann-Whitney t test; *p < 0.05, **p < 0.01.

E6-specific immunity. Furthermore, even though viral spread can be limited by the generation of antiviral immune responses, the initial local tumor cell killing may reverse the immunosuppressive tumor microenvironment, resulting in more effective antigen presentation and immune effector cell recruitment.[53] We are also investigating the effect of combining VSV-M51R-E7/6 therapy with checkpoint inhibitors[53–56] and with adoptive transfer of stem or central memory T cells.[57–59]

In summary, we have compared several different VSV-based vectors for the immunovirotherapy of HPV[POS] cancers. Based on the efficacy/toxicity profiles of these platforms, VSV-M51R-E7/6 looks most promising for clinical evaluation into a first-in-human phase I clinical trial, where virus will be simultaneously administered both i.v. and i.t. to optimize the combination of oncolytic and tumor-specific immunostimulatory properties.

MATERIALS AND METHODS

Cell Culture and Assays

All cell lines were cultured at 37°C in 5% CO_2 atmosphere and tested negative for mycoplasma contamination. BHK-21, MPC-11, LoVo, and HT1080 cells were purchased from the American Type Culture Collection (ATCC, Manassas, VA). TC-1 cells were obtained from T.C. Wu (Johns Hopkins, MD). Human primary HEKa cells were purchased from Gibco. Mel624 were provided by Mayo Clinic. *In vitro* growth curves were as follows: BHK-21 and TC-1 cells were incubated with recombinant VSV at a MOI of 0.002 (for BHK-21 cells) or 0.1 (for TC-1 cells). Two replicates in 10-cm plates were used for each HPV E7/6-expressing virus, and one replicate plate was used for each control virus (20 plates total). After 1 hr of incubation, the inoculums were removed, the cells were washed once with Dulbecco's PBS (DPBS), and fresh growth media was placed on the cells. At 12, 24, 48, and 72 hr after infection, virus-containing supernatant was harvested from each plate and

Multiple clinical trials are currently under way testing the safety and efficacy of many oncolytic viruses, and talimogene laherparepvec (T-VEC) has been FDA approved for melanoma treatment. Viruses are efficient in generating a "hot" inflammatory milieu in the tumor microenviroment, with cell killing resulting in the release of tumor and viral antigens that may stimulate a broader adaptive immunity, including responses directed toward tumor neoantigens.[49–51] In addition, it was recently reported that in two patients with complete remissions of HPV[POS] cervical cancer after immunotherapy, the T cell landscape consisted of both HPV-specific and non-viral tumor-antigen-specific T cells.[52] Therefore, the direct oncolytic properties of VSV-M51R-E7/6 in theory could also generate a more diverse and potent tumor-specific immunity in addition to HPV16 E7- and

A

B

Logrank P-value	Saline			
VSV-M51R-E7/6	0.0007	VSV-M51R-E7/6		
VSV-M51R-E7/6 + Anti-CD8	0.9299	0.0006	VSV-M51R-E7/6 + Anti-CD8	
VSV-M51R-E7/6 + Anti-CD4	<0.0001	0.0359	<0.0001	VSV-M51R-E7/6 + Anti-CD4
VSV-M51R-E7/6 + Anti-NK	<0.0001	0.7868	<0.0001	0.6200

VSV-M51R-E7/6 + Anti-NK
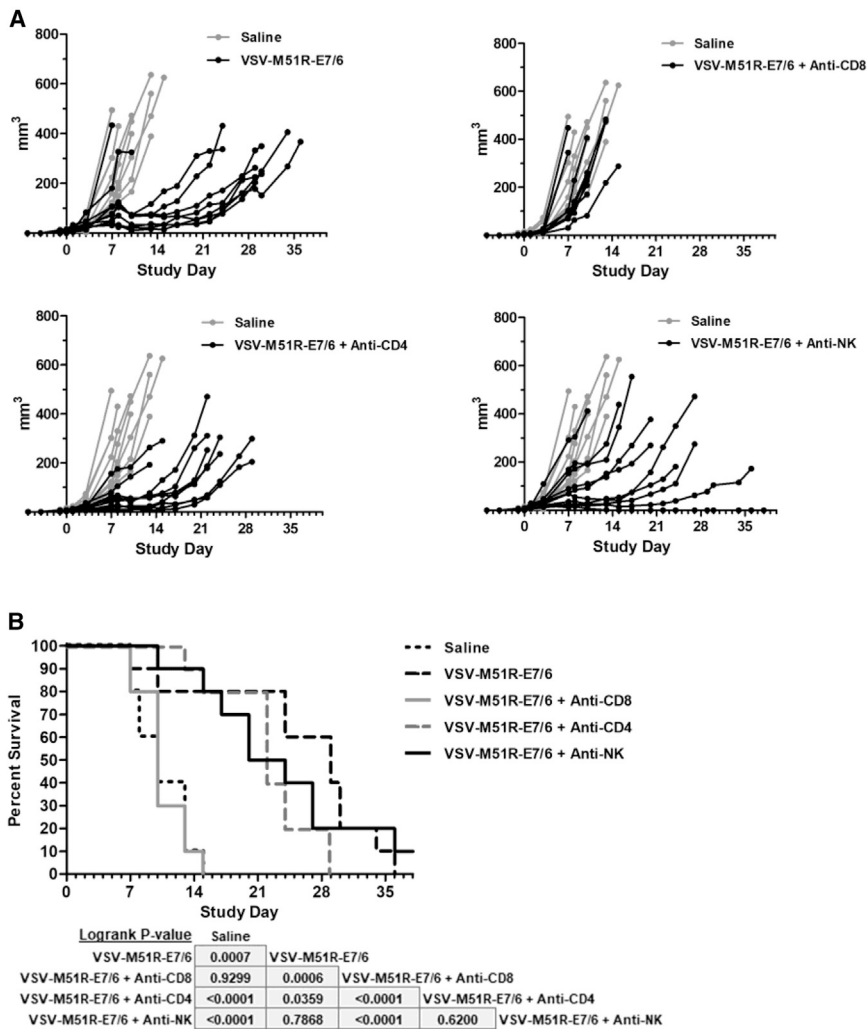
Figure 8. VSV-M51R-E7/6 Efficacy in the TC-1 Tumor Model Is Dependent on the Generation of a CD8⁺ T Cell Response

(A) Tumor volume measurements and (B) Kaplan-Meier survival curves of VSV-M51R-E7/6 treated C57BL/6 (n = 10) mice bearing TC-1 tumors after depletion of different subsets of immune cells. Mice were treated intraperitoneally with depleting antibodies (200 μg/mouse) starting 4 days after tumor implantation and twice weekly thereafter (100 μg/mouse). Mice received a concomitant i.v. and i.t. injection of VSV-M51R-E7/6 (5 × 10⁸ TCID₅₀ total dose, splitting the dose in half for concomitant i.v. and i.t. injection) or saline, starting 7 days after tumor implantation. Kaplan-Meier survival curves were compared by log rank (Mantel-Cox) analysis. A value of p < 0.05 was considered statistically significant.

bility of internal translation initiation of the E6 protein. The E6 protein sequence (151 aa) within the E7/6 fusion protein represents the smaller of two putative E6 ORFs[60,61] in the published genomic sequence (nt 83–559 and nt 104–559). To inactivate oncogenic potential of E7 and E6 proteins, five single point mutations in the E7/6 fusion gene were introduced by site-directed mutagenesis.[28] Each mutation results in a single amino acid substitution, three affecting the E7 and two the E6 protein. In E6, the mutations disrupt both zinc-finger domains, which are important for protein structure and function.

Cloning and Rescue of Recombinant VSV

The HPV PM E7/6 fusion cDNA was PCR amplified from plasmid pPBS-HPV-003. N gene translocation and G truncation in VSV-E7/6-N4CT9 were performed as previously described.[30,62] To generate pVSV-MC11-E7/6, the HPV16 PM E7/6 fusion cDNA was PCR amplified and inserted into the pVSV-MC11 vector after the M gene. Subsequent site-directed mutagenesis (Quickchange lightning mutagenesis kit; Agilent Technologies) was used to introduce the M51R mutation, generating pVSV-MC11-M51R-E7/6. To generate pVSV-MC11-E7/6-mIFNβ and pVSV-MC11-E7/6-hIFNβ, the mIFNβ and hIFNβ cDNAs, respectively, were PCR amplified and inserted into pVSV-MC11-E7/6 after the G gene. Recovery of VSV from the plasmid constructs was performed as previously described[63,64] with the use of a Vaccinia virus expressing the T7 polymerase (Imanis, #REA006). BHK-21 cells were used for production of viral particles. Virus identity was confirmed by sequencing the transgenic regions of the passage 2 viruses.

Western Blot

BHK-21 cells were plated on 6-well plates and infected with each virus (MOI = 3). Nine hours after infection, virus-infected cells

frozen at −80°C. The virus titer in each sample was determined by TCID₅₀ assay on BHK-21 cells. *In vitro* tumor-killing activity was as follows: TC-1 and MPC-11 cells were seeded in 96-well plates, and 12 hr later infected with VSV at MOIs of 10, 1, and 0.1 (for TC-1 cells) or 1, 0.1, and 0.01 (for MPC-11 cells). Mock-infected cells were used as a control. All conditions were assayed in triplicate. Cell viability was determined 48 or 72 hr after infection using a CellTiter 96 AQueous One Solution Cell Proliferation Assay (Promega, Madison, WI) following the manufacturer's protocol.

Fusion E7/6 Protein

The HPV16 E6 and E7 genes were derived from the plasmid DNA template pHPV-16 (ATCC, cat. #45113). The corresponding complete genomic sequence is published in NCBI GenBank, accession number K02718. First, the E6 and E7 genes were fused to generate a 747-bp-long open reading frame (ORF) encoding 248 aa. The E7 part of the E7/6 fusion protein (98 aa) remained unchanged, whereas the methionine start codon of the E6 ORF was removed to eliminate any possi-

were harvested with 250 μL of radioimmunoprecipitation assay (RIPA) buffer (25 mM Tris-HCl [pH 7.6], 150 mM NaCl, 1% NP-40, 1% sodium deoxycholate, 0.1% SDS) and incubated on ice for 10 min. Cell lysates were centrifuged, and the supernatants were collected and stored at −20°C until use. 5 μg protein was run on a Bolt 4%–12% Bis-Tris Plus gel (Thermo Fisher Scientific, Rockford, IL, cat #NW04125BOX) and transferred onto nitrocellulose membranes. After blocking for 1 hr with 3% skim milk-Tris-buffered saline (TBS)-Tween, membranes were blotted with primary antibodies against E7 (HPV Type 16 E7 monoclonal antibody [8C9], Thermo Fisher Scientific, Rockford, IL, cat. #28-0006) or VSV (a kind gift from Dr. Ammayappan, Mayo Clinic). After secondary staining with anti-rabbit or anti-mouse peroxidase-conjugated antibodies (Genesee Scientific, San Diego, CA, cat. #20-303 and Advansta, Menlo Park, CA, cat. #R-05071, respectively), protein bands were visualized on ProSignal Dura (Genesee Scientific, San Diego, CA, cat #20-301) chemiluminescence kit as recommended by the manufacturer.

In Vivo Experiments in Mice

All the experiments were approved by the Mayo Clinic Institutional Animal Care and Use Committee (IACUC). C57BL/6 mice or BALB/c (females 5 to 6 weeks old, Envigo, Indianapolis, IN) were implanted subcutaneously on the right hind flank with 2×10^5 TC-1 or 5×10^6 MPC-11 cells in 100 μL per mouse on the right hind flank. Mice were identified by microchip and ear notch, monitored for tumor growth, and were randomized into study groups when tumors reached a diameter of 2–3 mm. Mice were observed daily on days 0–4 for clinical signs. Tumor volumes and clinical observations were recorded at least three times per week until the end of each study or euthanasia of the mice. For depletion studies, mice were treated intraperitoneally with antibodies (BioXCell, West Lebanon, NH, 200 μg/mouse) starting 4 days after tumor implantation and twice weekly thereafter (100 μg/mouse). Clone 53-6.7 was used for CD8 T cell depletions, GK1.5 for CD4 T cells, and PK136 for NK1.1 cells. The GraphPad Prism 5.0 program (GraphPad Software, La Jolla, CA) was used for data handling, analysis, and graphic representation. Kaplan-Meier survival curves were compared by log rank (Mantel-Cox) analysis. A value of p < 0.05 was considered statistically significant.

Analysis for Hematological, Clinical Chemistry, and Biochemical Parameters

Blood was collected by cardiac puncture prior to necropsy. For clinical chemistry, 200 μL was collected in lithium heparin tubes (BD Diagnostic Systems, Sparks, MD); for complete blood count (CBC), 100 μL was collected in EDTA tubes (BD Diagnostic Systems, Sparks, MD); for RNA extraction, 100 μL was collected in RNA protect animal blood tubes (QIAGEN, MD); for serum, 600 μL was collected in serum separator tubes (BD Diagnostic Systems, Sparks, MD). Blood chemistry was analyzed using the ABAXIS Piccolo Xpress (Union City, CA), and CBC was done using the ABAXIS VetScan HM5 hematology machines. Clotting times were determined using the Coag Dx Analyzer (IDEXX VetLab Station, Westbrook, ME).

Murine IFNγ ELISPOT Assays

Mouse spleens were homogenized by grinding the spleens between the frosted ends of two sterile microscope slides. The resulting homogenate was suspended in 10 mL of complete R10 culture medium (RPMI-1640 containing 10% fetal bovine serum [FBS] and 2 mM L-glutamine, 100 U/mL penicillin, 100 μg/mL streptomycin sulfate, 1 mM sodium pyruvate, 1 mM HEPES, 100 μM non-essential amino acids) and ground into single cells. The splenocytes were subsequently isolated by Ficoll-Hypaque density gradient centrifugation and resuspended for 24 hr in complete R10 culture medium containing either 1 mg/mL concavalin-A (Con-A; Sigma), 2 mg/mL of HPV16 E7 and E6, as well as VSV N peptide pools, consisting of 15-mer peptides with 11-mer overlap, covering the entire protein sequence of HPV16 E7, E6, and VSV N. Splenocytes cultured with medium alone were used as control. Input cell numbers were 4×10^5. Input splenocytes per well were assayed in duplicate wells using a mouse IFNγ ELISPOT kit (BD Biosciences, San Diego, CA). The resulting spots were counted using an Immunospot Reader (CTL, Cleveland, OH). Peptide pool-specific IFNγ [no hyphen, also with beta] responses were considered positive if the response (minus media background) was ≥ 3 fold above the media response and ≥ 50 SFC/10^6 splenocytes.

Flow Cytometry

Tumor cell suspensions were treated for 5 min on ice with ammonium-chloride-potassium lysis (ACK) buffer (Invitrogen, CA), then tumor cells (5×10^5 to 1×10^6) were stained for 20 min in the dark at 4°C with surface marker monoclonal antibodies: rat anti-mouse CD45-PE, hamster anti-mouse CD3-V450, rat anti-mouse CD4-Alexa 700, and rat anti-mouse CD8-APC-Cy7. All antibodies were purchased from BD Biosciences. Cells were subsequently fixed in stabilizing fixative buffer (BD Biosciences) and stored at 4°C in the dark until flow cytometric analysis (performed within 24 hr). Data was collected using an LSRFortessa flow cytometer (BD Biosciences) configured to detect 12 fluorochromes, and analysis was performed using FlowJo software (version 10.0; TreeStar). Initial gating used forward scatter (FSC-A) versus SSC-A plot to remove cell debris. Leukocytes were selected with CD45$^+$ cells in CD45 versus FSC-A plot. T cells were selected by gating on CD3$^+$ cells in CD3 versus SSC-A plot; those T cells were further selected CD8$^+$ T cells by gating on CD4-CD8$^+$ T cells and selected CD4$^+$ T cells by gating on CD4$^+$CD8$^-$ T cells.

CONFLICTS OF INTEREST

S.J.R. and K.W.P. are chief executive officer and chief technology officer, respectively, at Vyriad. S.J.R., K.W.P., and Mayo Clinic hold equity in Vyriad.

REFERENCES

1. de Martel, C., Plummer, M., Vignat, J., and Franceschi, S. (2017). Worldwide burden of cancer attributable to HPV by site, country and HPV type. Int. J. Cancer *141*, 664–670.

2. Argiris, A., Harrington, K.J., Tahara, M., Schulten, J., Chomette, P., Ferreira Castro, A., and Licitra, L. (2017). Evidence-based treatment options in recurrent and/or metastatic squamous cell carcinoma of the head and neck. Front. Oncol. *7*, 72.

3. Borcoman, E., and Le Tourneau, C. (2017). Pembrolizumab in cervical cancer: latest evidence and clinical usefulness. Ther. Adv. Med. Oncol. *9*, 431–439.

4. Ott, P.A., Piha-Paul, S.A., Munster, P., Pishvaian, M.J., van Brummelen, E.M.J., Cohen, R.B., Gomez-Roca, C., Ejadi, S., Stein, M., Chan, E., et al. (2017). Safety and antitumor activity of the anti-PD-1 antibody pembrolizumab in patients with recurrent carcinoma of the anal canal. Ann. Oncol. *28*, 1036–1041.

5. Morris, V.K., Salem, M.E., Nimeiri, H., Iqbal, S., Singh, P., Ciombor, K., Polite, B., Deming, D., Chan, E., Wade, J.L., et al. (2017). Nivolumab for previously treated unresectable metastatic anal cancer (NCI9673): a multicentre, single-arm, phase 2 study. Lancet Oncol. *18*, 446–453.

6. Klingelhutz, A.J., and Roman, A. (2012). Cellular transformation by human papillomaviruses: lessons learned by comparing high- and low-risk viruses. Virology *424*, 77–98.

7. Yang, A., Farmer, E., Wu, T.C., and Hung, C.F. (2016). Perspectives for therapeutic HPV vaccine development. J. Biomed. Sci. *23*, 75.

8. Fountzilas, C., Patel, S., and Mahalingam, D. (2017). Review: Oncolytic virotherapy, updates and future directions. Oncotarget *8*, 102617–102639.

9. Lawler, S.E., Speranza, M.C., Cho, C.F., and Chiocca, E.A. (2017). Oncolytic viruses in cancer treatment. A review. JAMA Oncol. *3*, 841–849.

10. Barber, G.N. (2004). Vesicular stomatitis virus as an oncolytic vector. Viral Immunol. *17*, 516–527.

11. Lichty, B.D., Power, A.T., Stojdl, D.F., and Bell, J.C. (2004). Vesicular stomatitis virus: re-inventing the bullet. Trends Mol. Med. *10*, 210–216.

12. Melzer, M.K., Lopez-Martinez, A., and Altomonte, J. (2017). Oncolytic vesicular stomatitis virus as a viro-immunotherapy: Defeating cancer with a "hammer" and "anvil". Biomedicines *5*, 8.

13. Jenks, N., Myers, R., Greiner, S.M., Thompson, J., Mader, E.K., Greenslade, A., Griesmann, G.E., Federspiel, M.J., Rakela, J., Borad, M.J., et al. (2010). Safety studies on intrahepatic or intratumoral injection of oncolytic vesicular stomatitis virus expressing interferon-beta in rodents and nonhuman primates. Hum. Gene Ther. *21*, 451–462.

14. Zhang, L., Steele, M.B., Jenks, N., Grell, J., Suksanpaisan, L., Naik, S., Federspiel, M.J., Lacy, M.Q., Russell, S.J., and Peng, K.W. (2016). Safety studies in tumor and non-tumor-bearing mice in support of clinical trials using oncolytic VSV-IFNβ-NIS. Hum. Gene Ther. Clin. Dev. *27*, 111–122.

15. Naik, S., Galyon, G.D., Jenks, N.J., Steele, M.B., Miller, A.C., Allstadt, S.D., Suksanpaisan, L., Peng, K.W., Federspiel, M.J., Russell, S.J., and LeBlanc, A.K. (2018). Comparative oncology evaluation of intravenous recombinant oncolytic vesicular stomatitis virus therapy in spontaneous canine cancer. Mol. Cancer Ther. *17*, 316–326.

16. Liao, J.B., Publicover, J., Rose, J.K., and DiMaio, D. (2008). Single-dose, therapeutic vaccination of mice with vesicular stomatitis virus expressing human papillomavirus type 16 E7 protein. Clin. Vaccine Immunol. *15*, 817–824.

17. Diaz, R.M., Galivo, F., Kottke, T., Wongthida, P., Qiao, J., Thompson, J., Valdes, M., Barber, G., and Vile, R.G. (2007). Oncolytic immunovirotherapy for melanoma using vesicular stomatitis virus. Cancer Res. *67*, 2840–2848.

18. Bridle, B.W., Boudreau, J.E., Lichty, B.D., Brunellière, J., Stephenson, K., Koshy, S., Bramson, J.L., and Wan, Y. (2009). Vesicular stomatitis virus as a novel cancer vaccine vector to prime antitumor immunity amenable to rapid boosting with adenovirus. Mol. Ther. *17*, 1814–1821.

19. Pulido, J., Kottke, T., Thompson, J., Galivo, F., Wongthida, P., Diaz, R.M., Rommelfanger, D., Ilett, E., Pease, L., Pandha, H., et al. (2012). Using virally expressed melanoma cDNA libraries to identify tumor-associated antigens that cure melanoma. Nat. Biotechnol. *30*, 337–343.

20. Atherton, M.J., Stephenson, K.B., Pol, J., Wang, F., Lefebvre, C., Stojdl, D.F., Nikota, J.K., Dvorkin-Gheva, A., Nguyen, A., Chen, L., et al. (2017). Customized viral immunotherapy for HPV-associated cancer. Cancer Immunol. Res. *5*, 847–859.

21. Bosch, F.X., Manos, M.M., Muñoz, N., Sherman, M., Jansen, A.M., Peto, J., Schiffman, M.H., Moreno, V., Kurman, R., and Shah, K.V. (1995). Prevalence of human papillomavirus in cervical cancer: a worldwide perspective. International biological study on cervical cancer (IBSCC) Study Group. J. Natl. Cancer Inst. *87*, 796–802.

22. Gillison, M.L., D'Souza, G., Westra, W., Sugar, E., Xiao, W., Begum, S., and Viscidi, R. (2008). Distinct risk factor profiles for human papillomavirus type 16-positive and human papillomavirus type 16-negative head and neck cancers. J. Natl. Cancer Inst. *100*, 407–420.

23. Hansson, B.G., Rosenquist, K., Antonsson, A., Wennerberg, J., Schildt, E.B., Bladström, A., and Andersson, G. (2005). Strong association between infection with human papillomavirus and oral and oropharyngeal squamous cell carcinoma: a population-based case-control study in southern Sweden. Acta Otolaryngol. *125*, 1337–1344.

24. D'Souza, G., Gross, N.D., Pai, S.I., Haddad, R., Anderson, K.S., Rajan, S., Gerber, J., Gillison, M.L., and Posner, M.R. (2014). Oral human papillomavirus (HPV) infection in HPV-positive patients with oropharyngeal cancer and their partners. J. Clin. Oncol. *32*, 2408–2415.

25. Dalal, S., Gao, Q., Androphy, E.J., and Band, V. (1996). Mutational analysis of human papillomavirus type 16 E6 demonstrates that p53 degradation is necessary for immortalization of mammary epithelial cells. J. Virol. *70*, 683–688.

26. Gao, Q., Singh, L., Kumar, A., Srinivasan, S., Wazer, D.E., and Band, V. (2001). Human papillomavirus type 16 E6-induced degradation of E6TP1 correlates with its ability to immortalize human mammary epithelial cells. J. Virol. *75*, 4459–4466.

27. Münger, K., Basile, J.R., Duensing, S., Eichten, A., Gonzalez, S.L., Grace, M., and Zacny, V.L. (2001). Biological activities and molecular targets of the human papillomavirus E7 oncoprotein. Oncogene *20*, 7888–7898.

28. Cassetti, M.C., McElhiney, S.P., Shahabi, V., Pullen, J.K., Le Poole, I.C., Eiben, G.L., Smith, L.R., and Kast, W.M. (2004). Antitumor efficacy of Venezuelan equine encephalitis virus replicon particles encoding mutated HPV16 E6 and E7 genes. Vaccine *22*, 520–527.

29. Iverson, L.E., and Rose, J.K. (1981). Localized attenuation and discontinuous synthesis during vesicular stomatitis virus transcription. Cell *23*, 477–484.

30. Clarke, D.K., Nasar, F., Lee, M., Johnson, J.E., Wright, K., Calderon, P., Guo, M., Natuk, R., Cooper, D., Hendry, R.M., and Udem, S.A. (2007). Synergistic attenuation of vesicular stomatitis virus by combination of specific G gene truncations and N gene translocations. J. Virol. *81*, 2056–2064.

31. Randle, R.W., Northrup, S.A., Sirintrapun, S.J., Lyles, D.S., and Stewart, J.H., 4th (2013). Oncolytic vesicular stomatitis virus as a treatment for neuroendocrine tumors. Surgery *154*, 1323–1329, discussion 1329–1330.

32. Blackham, A.U., Northrup, S.A., Willingham, M., Sirintrapun, J., Russell, G.B., Lyles, D.S., and Stewart, J.H., 4th (2014). Molecular determinants of susceptibility to oncolytic vesicular stomatitis virus in pancreatic adenocarcinoma. J. Surg. Res. *187*, 412–426.

33. Ahmed, M., McKenzie, M.O., Puckett, S., Hojnacki, M., Poliquin, L., and Lyles, D.S. (2003). Ability of the matrix protein of vesicular stomatitis virus to suppress beta interferon gene expression is genetically correlated with the inhibition of host RNA and protein synthesis. J. Virol. *77*, 4646–4657.

34. Obuchi, M., Fernandez, M., and Barber, G.N. (2003). Development of recombinant vesicular stomatitis viruses that exploit defects in host defense to augment specific oncolytic activity. J. Virol. *77*, 8843–8856.

35. Zhang, L., Steele, M.B., Jenks, N., Grell, J., Behrens, M., Nace, R., Naik, S., Federspiel, M.J., Russell, S.J., and Peng, K.W. (2016). Robust oncolytic virotherapy induces tumor lysis syndrome and associated toxicities in the MPC-11 plasmacytoma model. Mol. Ther. *24*, 2109–2117.

36. Lin, K.Y., Guarnieri, F.G., Staveley-O'Carroll, K.F., Levitsky, H.I., August, J.T., Pardoll, D.M., and Wu, T.C. (1996). Treatment of established tumors with a novel vaccine that enhances major histocompatibility class II presentation of tumor antigen. Cancer Res. 56, 21–26.

37. Coller, B.G., Blue, J., Das, R., Dubey, S., Finelli, L., Gupta, S., Helmond, F., Grant-Klein, R.J., Liu, K., Simon, J., et al. (2017). Clinical development of a recombinant Ebola vaccine in the midst of an unprecedented epidemic. Vaccine 35 (35 Pt A), 4465–4469.

38. Holay, N., Kim, Y., Lee, P., and Gujar, S. (2017). Sharpening the edge for precision cancer immunotherapy: targeting tumor antigens through oncolytic vaccines. Front. Immunol. 8, 800.

39. Le Bon, A., and Tough, D.F. (2008). Type I interferon as a stimulus for cross-priming. Cytokine Growth Factor Rev. 19, 33–40.

40. Corrales, L., and Gajewski, T.F. (2016). Endogenous and pharmacologic targeting of the STING pathway in cancer immunotherapy. Cytokine 77, 245–247.

41. Fuchs, J.D., Frank, I., Elizaga, M.L., Allen, M., Frahm, N., Kochar, N., Li, S., Edupuganti, S., Kalams, S.A., Tomaras, G.D., et al. (2015). First-in-human evaluation of the safety and immunogenicity of a recombinant vesicular stomatitis virus human immunodeficiency virus-1 gag vaccine (HVTN 090). Open Forum Infect. Dis. 2, ofv082.

42. Henao-Restrepo, A.M., Longini, I.M., Egger, M., Dean, N.E., Edmunds, W.J., Camacho, A., Carroll, M.W., Doumbia, M., Draguez, B., Duraffour, S., et al. (2015). Efficacy and effectiveness of an rVSV-vectored vaccine expressing Ebola surface glycoprotein: interim results from the Guinea ring vaccination cluster-randomised trial. Lancet 386, 857–866.

43. Johnson, J.E., Coeman, J.W., Narender, K.K., Calderon, P., Wright, K.J., Obregon, J., Ogin-Wilson, E., Natuk, R.J., Clarke, D.K., Udem, S.A., et al. (2009). In vivo biodistribution of a highly attenuated recombinant vesicular stomatitis virus expressing Hi.v.-1 gag following intramuscular, intranasal or intravenous inoculation. Vaccine 27, 2930–2939.

44. Barouch, D.H., Pau, M.G., Custers, J.H., Koudstaal, W., Kostense, S., Havenga, M.J., Truitt, D.M., Sumida, S.M., Kishko, M.G., Arthur, J.C., et al. (2004). Immunogenicity of recombinant adenovirus serotype 35 vaccine in the presence of pre-existing anti-Ad5 immunity. J. Immunol. 172, 6290–6297.

45. Casimiro, D.R., Chen, L., Fu, T.M., Evans, R.K., Caulfield, M.J., Davies, M.E., Tang, A., Chen, M., Huang, L., Harris, V., et al. (2003). Comparative immunogenicity in rhesus monkeys of DNA plasmid, recombinant vaccinia virus, and replication-defective adenovirus vectors expressing a human immunodeficiency virus type 1 gag gene. J. Virol. 77, 6305–6313.

46. Santra, S., Sun, Y., Parvani, J.G., Philippon, V., Wyand, M.S., Manson, K., Gomez-Yafal, A., Mazzara, G., Panicali, D., Markham, P.D., et al. (2007). Heterologous prime/boost immunization of rhesus monkeys by using diverse poxvirus vectors. J. Virol. 81, 8563–8570.

47. Tober, R., Banki, Z., Egerer, L., Muik, A., Behmüller, S., Kreppel, F., Greczmiel, U., Oxenius, A., von Laer, D., and Kimpel, J. (2014). VSV-GP: a potent viral vaccine vector that boosts the immune response upon repeated applications. J. Virol. 88, 4897–4907.

48. Lee, S.Y., Kang, T.H., Knoff, J., Huang, Z., Soong, R.S., Alvarez, R.D., Hung, C.F., and Wu, T.C. (2013). Intratumoral injection of therapeutic HPV vaccinia vaccine following cisplatin enhances HPV-specific antitumor effects. Cancer Immunol. Immunother. 62, 1175–1185.

49. Russell, S.J., and Peng, K.W. (2017). Oncolytic virotherapy: a contest between apples and oranges. Mol Ther. 25, 1107–1116.

50. Coffin, R.S. (2016). Oncolytic immunotherapy: an emerging new modality for the treatment of cancer. Ann. Oncol. 27, 1805–1808.

51. Woller, N., Gürlevik, E., Fleischmann-Mundt, B., Schumacher, A., Knocke, S., Kloos, A.M., Saborowski, M., Geffers, R., Manns, M.P., Wirth, T.C., et al. (2015). Viral infection of tumors overcomes resistance to PD-1-immunotherapy by broadening neoantigenome-directed T-cell Responses. Mol. Ther. 23, 1630–1640.

52. Stevanović, S., Pasetto, A., Helman, S.R., Gartner, J.J., Prickett, T.D., Howie, B., Robins, H.S., Robbins, P.F., Klebanoff, C.A., Rosenberg, S.A., and Hinrichs, C.S. (2017). Landscape of immunogenic tumor antigens in successful immunotherapy of virally induced epithelial cancer. Science 356, 200–205.

53. Gujar, S., Pol, J.G., Kim, Y., Lee, P.W., and Kroemer, G. (2018). Antitumor benefits ofantiviral immunity: an underappreciated aspect of oncolytic virotherapies. Trends Immunol 39, 209–221.

54. Shen, W., Patnaik, M.M., Ruiz, A., Russell, S.J., and Peng, K.W. (2016). Immunovirotherapy with vesicular stomatitis virus and PD-L1 blockade enhances therapeutic outcome in murine acute myeloid leukemia. Blood 127, 1449–1458.

55. Zamarin, D., Holmgaard, R.B., Subudhi, S.K., Park, J.S., Mansour, M., Palese, P., Merghoub, T., Wolchok, J.D., and Allison, J.P. (2014). Localized oncolytic virotherapy overcomes systemic tumor resistance to immune checkpoint blockade immunotherapy. Sci. Transl. Med. 6, 226ra32.

56. Ribas, A., Dummer, R., Puzanov, I., VanderWalde, A., Andtbacka, R.H.I., Michielin, O., Olszanski, A.J., Malvehy, J., Cebon, J., Fernandez, E., et al. (2017). Oncolytic virotherapy promotes intratumoral T cell infiltration and improves anti-PD-1 immunotherapy. Cell 170, 1109–1119.e10.

57. Wongthida, P., Diaz, R.M., Pulido, C., Rommelfanger, D., Galivo, F., Kaluza, K., Kottke, T., Thompson, J., Melcher, A., and Vile, R. (2011). Activating systemic T-cell immunity against self tumor antigens to support oncolytic virotherapy with vesicular stomatitis virus. Hum. Gene Ther. 22, 1343–1353.

58. Rommelfanger, D.M., Wongthida, P., Diaz, R.M., Kaluza, K.M., Thompson, J.M., Kottke, T.J., and Vile, R.G. (2012). Systemic combination virotherapy for melanoma with tumor antigen-expressing vesicular stomatitis virus and adoptive T-cell transfer. Cancer Res. 72, 4753–4764.

59. Ramos, C.A., Narala, N., Vyas, G.M., Leen, A.M., Gerdemann, U., Sturgis, E.M., Anderson, M.L., Savoldo, B., Heslop, H.E., Brenner, M.K., and Rooney, C.M. (2013). Human papillomavirus type 16 E6/E7-specific cytotoxic T lymphocytes for adoptive immunotherapy of HPV-associated malignancies. J. Immunother. 36, 66–76.

60. Seedorf, K., Krämmer, G., Dürst, M., Suhai, S., and Röwekamp, W.G. (1985). Human papillomavirus type 16 DNA sequence. Virology 145, 181–185.

61. Smotkin, D., and Wettstein, F.O. (1986). Transcription of human papillomavirus type 16 early genes in a cervical cancer and a cancer-derived cell line and identification of the E7 protein. Proc. Natl. Acad. Sci. USA 83, 4680–4684.

62. Schnell, M.J., Buonocore, L., Boritz, E., Ghosh, H.P., Chernish, R., and Rose, J.K. (1998). Requirement for a non-specific glycoprotein cytoplasmic domain sequence to drive efficient budding of vesicular stomatitis virus. EMBO J. 17, 1289–1296.

63. Lawson, N.D., Stillman, E.A., Whitt, M.A., and Rose, J.K. (1995). Recombinant vesicular stomatitis viruses from DNA. Proc. Natl. Acad. Sci. USA 92, 4477–4481.

64. Schnell, M.J., Buonocore, L., Whitt, M.A., and Rose, J.K. (1996). The minimal conserved transcription stop-start signal promotes stable expression of a foreign gene in vesicular stomatitis virus. J. Virol. 70, 2318–2323.